

# NON-LINEAR CONVECTION IN A POROUS MEDIUM WITH CONVECTIVE ACCELERATION AND VISCOUS FORCE

N. Rudraiah

UGC–DSA Centre in Fluid Mechanics,  
Department of Mathematics, Central College,  
Bangalore University, Bangalore–560001, India

الخلاصة :

ندرس في هذا البحث النقل الحرارى الغير خطى في وسط منفذ له تسارع نقل حرارى وقوة لزوجة ونفاذيته قريبة من الوحدة ، وذلك باستخدام تكامل القوة والتحليل الطيفي والتكنيكات العددية . ونلقى الضؤ على الكنير من التشابهات والاختلافات النوعية بين التكنيكات التحليلية ونستعمل في التكنيك العددي الرموز أودى ، آركي أف ٤٥ ، آركي أف ٤٨ لايجاد تكامل نظام المعادلات التفاضلية لمعاملات كاليركن (Galerkin). ولقد وجدنا أن بعض التمثيلات وأعداد رايلي (Rayleigh) الكبيرة جدا تعطى حلولاً مشوشة . كذلك بينا أن النفاذية تؤثر في شكل الخلية وتحد من تتابع النقل الحرارى . وهذا التأثير يشبه تأثير المجال المغناطيس على النقل في موضوع ديناميكا السوائل المغناطيسية .

## ABSTRACT

Non-linear convection in a porous medium of porosity close to unity with convective acceleration and viscous force is studied using power integral, spectral analysis and numerical techniques. Several similarities and qualitative differences between the analytical techniques are brought out. In the numerical technique, the codes ODE, RKF45, and RKF48 are used to integrate the system of differential equations for the Galerkin coefficients. It is found that certain representations and too high Rayleigh numbers produce chaotic solutions. It is also shown that permeability influences the cell pattern and inhibits the onset of convection. This effect is analogous to the effect of a magnetic field on convection in magne to hydrodynamics, previously treated by the author.

## NON-LINEAR CONVECTION IN A POROUS MEDIUM WITH CONVECTIVE ACCELERATION AND VISCOUS FORCE

### 1. INTRODUCTION

The main object of this paper is to discuss the merits and demerits of the use of different techniques in applicable mathematics for the study of free convection in a special type of coarse porous medium of porosity close to unity (for example, a porous medium made of fibrous materials or the mushy zone in a rapidly freezing material regarded as a porous material of varying permeability). This study has generated considerable interest in recent years because of its importance in many branches of science and engineering, particularly in petroleum engineering, to remove small particles contained in gases: one of the simple and useful methods of removal will be by means of a fibrous porous medium, that is, a filter. It is also of interest in the nuclear industry, particularly in the evaluation of heat removal from a hypothetical accident in a nuclear reactor and to provide effective insulation. Here, the main purpose is to reduce heat transfer by means of open-pore insulators, such as glass fibers or rock fibrous material. In formulating this problem, we regard the special type of porous medium as an assemblage of sparse distribution of small identical spherical particles of radius  $d_p$  and number density  $\rho_p$  fixed in space. Since the porosity,  $\varphi = 1 - \frac{4}{3}\pi d_p^3 \rho_p$ , of the medium is close to unity, we choose  $d_p$  such that  $d_p^3 \rho_p \rightarrow 0$  while  $d_p \rho_p = \text{finite}$  when  $\rho_p \rightarrow \infty$ . In this type of porous medium, the macroscopic velocity is not always small and hence the inertial force may not be negligible. Further, the distortion of velocity gives rise to shear stresses which in turn give rise to a viscous force. Therefore, the study of convection in such a special type of coarse porous medium needs the generalized Darcy law which incorporates both inertial and viscous forces in addition to the usual Darcy resistance. We hope that it offers a quantitative theory for the details of the transition from the conduction regime to convection and a convenient means for demonstrating experimentally the non-linear effects such as the preferred cell pattern, heat transport, and so on.

Free convection in a porous medium heated from below has been extensively studied [1] using a linear pressure-velocity relation called Darcy's Law [2],

$$\mathbf{q} = -\frac{k}{\mu}(\nabla p - \rho \mathbf{g}), \quad (1)$$

where  $\mathbf{q}$  is the mean filter velocity vector,  $\nabla p$  the pressure gradient,  $k$  the permeability of the medium,  $\mu$  the viscosity and  $\rho$  the density of the fluid, and  $\mathbf{g}$  is the acceleration due to gravity. This is usually called Rayleigh-Darcy (RD) convection which is analogous to Rayleigh-Benard convection. The Hele-Shaw [3] cell model with two parallel plates separated by a distance  $d$  in which the mean velocity vector [4] is

$$\mathbf{q} = -\frac{d^2}{12\mu}(\nabla p - \rho \mathbf{g}) \quad (2)$$

enables experimentalists to simulate the flow through a porous medium [5]. This hydraulic analogy of the Hele-Shaw cell model is rigorous for isothermal flow when an equivalent permeability  $k = \frac{d^2}{12}$  is defined. It has been suggested that convection in Hele-Shaw cells could be characterized by a single, properly defined Rayleigh number [6, 7]

$$R_L = \frac{\alpha g \Delta T d k}{\nu \kappa^*} \quad (3)$$

called the filtration or Lapwood [7] Rayleigh number, where  $\kappa^*$  is the average thermal diffusivity,  $\alpha$  the coefficient of thermal expansion,  $\Delta T$  the temperature difference,  $\nu$  the kinematic viscosity,  $k$  the permeability of the medium, and  $d$  the width of the porous layer. Katto and Masuoka [8] and Elder [9, 10] have given a detailed theoretical analysis of various flows (which they also observed experimentally) using the average thermal diffusivity  $\kappa^* = \frac{K^*}{(\rho c)_f}$ , where  $K^*$  is the effective thermal conductivity of the saturated medium and  $(\rho c)_f$  is the thermal capacity of the fluid.  $K^*$  is a complex function of the solid and liquid thermal conductivities, as well as of some parameters such as the texture of the porous medium. A model to determine  $K^*$  is given in [8, 11]. Hartline and Lister [12, 13] carried out careful experiments to measure the critical Rayleigh number and the flow velocity of thermal convection in Hele-Shaw cells under supercritical conditions using  $K^* = \frac{K_f^* \varphi^* + (1 - \varphi^*) K_s^*}{(\rho c)_f}$ ,

where  $K_l^*$  and  $K_s^*$  are the thermal conductivity of the fluid and solid, respectively, and  $\varphi^* = d/h$ , where  $h$  is the width of the cells.

The investigations on convection in a porous medium discussed above are concerned only with low speed flows. However, it is well known that the flow of fluid in a porous medium is curvilinear and the curvature of the path gives rise to inertial acceleration. Further, in the special type of coarse porous medium discussed here, the speed of flow is not always small, so that inertial acceleration cannot be neglected [14–17]. Although Hamel [14] was the first to consider the inertial acceleration in the Darcy equation (1), Lapwood [7] gave a systematic mathematical analysis to study linear convection in a porous medium using the generalized Darcy equation

$$\rho \left[ \frac{\partial \mathbf{q}}{\partial t} + (\mathbf{q} \cdot \nabla) \mathbf{q} \right] = -\nabla p + \rho \mathbf{g} - \frac{\mu}{k} \mathbf{q} \quad (4)$$

which we call the Lapwood–Darcy (LD) equation. Subsequently, many authors [18–24] have used this equation to study linear and non-linear convection in a porous medium. The inclusion of inertial acceleration in the Darcy equation is usually valid for small values of the Prandtl number (for example, with liquid metals). But it poses, as pointed out by Beck [25], the problem of an under-specified system of equations when the basic state is not quiescent. We can overcome this difficulty by considering the Forchheimer [26] model where the usual inertial acceleration is expressed as a quadratic drag term. In that case the LD equation (4) takes the form

$$\rho \frac{\partial \mathbf{q}}{\partial t} = -\nabla p + \rho \mathbf{g} - \frac{\mu}{k} \mathbf{q} - \rho C_b |\mathbf{q}| \mathbf{q}, \quad (5)$$

where  $C_b$  is the drag parameter [27]. This form of generalized Darcy equation is called the Forchheimer–Darcy (FD) equation.

We note that one can overcome the problem of an under-specified system of equations arising from the LD equation (4) in the case of a non-quiescent state by considering the viscous force  $\mu \nabla^2 \mathbf{q}$  due to the distortion of velocity in addition to the inertial acceleration. The analysis of flow through a porous medium [15–17] using the LD equation shows that the vorticity emerges at the discontinuity surface of permeability when the fluid flows across the surface and it decays steadily in the flow when the permeability is constant. To account for this decay, we must consider the viscous force. Further, at the edge of the mushy zone next to a melt, the dendritic growths are widely

separated corresponding to large permeability where the Darcy friction  $-\frac{\mu}{k} \mathbf{q}$  becomes comparable to and even becomes considerably smaller than  $\mu \nabla^2 \mathbf{q}$ . The experiments of Stark and Volker [28] on the parallel plate Hele-Shaw model clearly demonstrate the existence of diffusion and convective acceleration. Therefore, a study of convection in a porous medium of porosity close to unity requires the viscous force  $\mu \nabla^2 \mathbf{q}$  in the LD equation (4). Recently, many authors [29–34] have generalized the Darcy equation, incorporating the inertial and viscous forces in addition to Darcy friction, to the form

$$\rho \left[ \frac{\partial \mathbf{q}}{\partial t} + (\mathbf{q} \cdot \nabla) \mathbf{q} \right] = -\nabla p + \rho \mathbf{g} - \frac{\mu}{k} \mathbf{q} + \mu \nabla^2 \mathbf{q}. \quad (6)$$

This reduces, for steady low Reynolds number flow, to the one proposed by Brinkman [35] for creeping flow past an individual sphere. Subsequently, many authors [29, 30, 36, 43] have shown that the Brinkman model gives, to the first approximation, results for flow through a porous medium made of a sparse distribution of spheres. Hereafter, (6) is called the Darcy–Lapwood–Brinkman (DLB) equation. This equation is used in this paper to study non-linear convection.

Recently, attention [37–41] has been focused on the study of convection in a porous medium using the DLB equation. The work in [37] is based on the energy method which predicts only the criterion for the onset of convection subject to arbitrary disturbances, and is silent about the prediction of cell pattern and the corresponding heat transfer. The work in [41] deals only with two-dimensional convection based on spectral analysis. Although this method predicts the cross-interaction of different modes, it is silent about the prediction of different cell patterns. Further, in [41], because of the prominence given to finite amplitude convection of odd parity, the even parity modes are excluded from the discussion of the linear convection problem. If the separation  $D$  of the vertical walls of the mode is small enough, the  $\gamma = (1, 1)$  mode enters first when the Rayleigh number  $R$  is adiabatically increased from zero, but if  $D$  is adiabatically increased, a stage will be reached when the  $\gamma = (2, 1)$  mode has a smaller  $R_c$  and then when convection first occurs it will be on a two cell pattern. By concentrating only on the odd parity modes, Rudraiah and Balachandra Rao [41] have ruled out this possibility. However, we overcome this deficiency in this paper. Finally, three-dimensional non-linear convection has not been given much attention using the DLB equation. This is also studied in this paper.

## 2. FORMULATION OF THE PROBLEM

Consider a Boussinesq fluid saturated porous layer occupying the space between two parallel horizontal planes of infinite extent separated by a distance  $d$ , heated uniformly from below and cooled from above. This means that we have a top-heavy arrangement and hence the equilibrium is unstable. However, the viscous friction and the thermal diffusion act to stabilize the system and create a threshold thermal gradient above which convection occurs and below which the fluid is in the quiescent state. The point at which the quiescent state breaks down and the motion starts is called the critical point and the corresponding temperature gradient is called the critical temperature gradient. This is expressed, in dimensionless form, in terms of the critical Rayleigh number  $R_c$ .

The DLB model with the usual approximations (see [21]) is introduced here to study the non-linear convection. In addition to this, models are also necessary to account for heat transfer. The simplest model considers that, at a given point, the fluid and solid phases are at the same temperature to form a fictitious fluid with a heat capacity

$$(\rho c)^* = (\rho c)_f \phi + (1 - \phi)(\rho c)_s \quad (7)$$

and the effective thermal conductivity  $K^*$ ; in (7),  $(\rho c)_f$  and  $(\rho c)_s$  are the heat capacities for the fluid and solid states, respectively.

### 2.1 Basic Equations

The required equations for a representative elementary volume under the Boussinesq approximation [42] are:

$$\nabla \cdot \mathbf{q} = 0 \quad (8)$$

$$\frac{\partial \mathbf{q}}{\partial t} + (\mathbf{q} \cdot \nabla) \mathbf{q} = -\frac{1}{\rho_0} \nabla p + \alpha \mathbf{g}(T - T_0) - \frac{\nu}{k} \mathbf{q} + \nu \nabla^2 \mathbf{q} \quad (9)$$

$$(\rho c)^* \frac{\partial T}{\partial t} + (\rho c)_f (\mathbf{q} \cdot \nabla) T = K^* \nabla^2 T, \quad (10)$$

$$\rho = \rho_0 [1 - \alpha(T - T_0)], \quad (11)$$

where 
$$\nabla^2 \equiv \frac{\partial^2}{\partial x^2} + \frac{\partial^2}{\partial y^2} + \frac{\partial^2}{\partial z^2},$$

and  $\mathbf{q} = (u, v, w)$  is the mean filter velocity,  $p$  the pressure,  $T$  the temperature,  $\rho$  the density,  $\rho_0$  the density at the reference  $T_0$ ,  $\nu$  the kinematic viscosity, and  $k$  the permeability.

## 3. NON-LINEAR CONVECTION USING THE POWER INTEGRAL TECHNIQUE

This is an iterative technique [22] which combines the best features of the Galerkin technique [43] and Stuart's [44] shape assumption. This method is capable of predicting the nature of the amplitude at a given value of the Rayleigh number, the energetics of the fluid, and the physically preferred motions for a given set of external parameters. The perturbations on the basic flow are assumed to be finite so that higher order terms in the stability equation have to be retained. It relies on a system of differential equations for each of the field variables. These are achieved by introducing parametric expansions of the motion and then equating the coefficients of each order of the parameter. From the zeroth order system of differential equations, corresponding to the linear theory, the form of one of the field variables is determined. Then we use Stuart's [44] shape assumption, which implies that the plan form that exists at the onset of convection (that is,  $R = R_c$ ) persists even after the onset of convection (that is,  $R > R_c$ , non-linear theory), to determine the remaining variables, where  $R = \frac{\alpha g \Delta T d^3}{\nu \kappa}$  is the Rayleigh number. The investigation of higher order approximations based on the solution to the linear stability problem is called local non-linear stability analysis. This analysis is useful to study in detail the possible horizontal patterns of closed packed cells, which are limited to two-dimensional rolls, rectangles, and hexagons.

To study the local non-linear convection, we assume that all the dependent variables, say  $f$  and  $R$ , vary in the form

$$f = f_0 \varepsilon + f_1 \varepsilon^2 + f_2 \varepsilon^3 + \dots \\ R = R_0 + \varepsilon R_1 + \varepsilon^2 R_2 + \dots, \quad (12)$$

where  $\varepsilon$  is a constant parameter and  $R_i$  are integral functions of  $w_i$  and  $T_i$ . For the first order solutions to be complete,  $\varepsilon$  must be proportional to the amplitude of the disturbance, and this amplitude must be infinitesimal.

Substituting (12) into (9) and (10) and equating the like powers of  $\varepsilon$ , we get the required equations (see [22]).

### 3.1 Analysis for Two-Dimensional Motion with a Free Surface

The first order solutions, satisfying the conditions

$$W = \frac{d^2 W}{dz^2} = T = 0, \quad \text{at } Z = 0 \text{ and } 1 \dots \quad (13)$$

are

$$\begin{aligned} u_0 &= -\frac{2}{a} \sin \pi ax \cos \pi z, \\ v_0 &= 0, \\ w_0 &= 2 \cos \pi ax \sin \pi z \end{aligned} \tag{14}$$

$$T_0 = 2 \frac{(a^2 + 1)}{a^2} \left\{ \pi^2(a^2 + 1) + \frac{1}{P_l} \right\} \cos \pi ax \sin \pi z, \tag{15}$$

$$R_0 = \frac{\pi^2(a^2 + 1)^2}{a^2} \left\{ \pi^2(a^2 + 1) + \frac{1}{P_l} \right\}, \tag{16}$$

$$P_l = k/d^2.$$

The lowest value of  $R_0$ , called the critical value  $(R_0)_c$ , occurs at  $a = a_c$ , where  $a_c$  satisfies the equation

$$2a^6 + \left( 3 + \frac{1}{\pi^2 P_l} \right) a^4 - \left( 1 + \frac{1}{\pi^2 P_l} \right) = 0. \tag{17}$$

It is of interest to note that, in the LD model, Rudraiah and Srimani [22] have shown that  $a$  is independent of  $P_l$  and takes the value unity. However, in the DLB model discussed here,  $a^2$  depends on  $P_l$  and hence the permeability influences the cell pattern. The critical values of  $(R_0)_c$  and  $a_c$  are computed from (16) and (17) for different values of  $P_l$  and the results are shown in Table 1.

**Table 1. Critical Values of  $R$  and  $a_c$**

$P_l$	$a_c^2$	$(R_0)_c$
$\infty$	0.5	$0.65875 \times 10^3$
$10^{-2}$	0.5306	$0.47191 \times 10^4$
$10^{-3}$	0.9636	$0.40290 \times 10^5$
$10^{-4}$	0.9961	$0.39588 \times 10^6$
$10^{-5}$	0.9959	$0.39518 \times 10^7$

From this table it is clear that in the limit of  $P_l \rightarrow \infty$  we recover the pure viscous flow results of Malkus and Veronis [45], and that for  $P_l \rightarrow 0$ , say  $P_l = 10^{-5}$ , we recover the LD model results [22]. For other values of  $P_l$ , in the range  $10^{-2} - 10^{-3}$ , we get the results for the transition zone from the DLB model to the LD model [44]. From Table 1 it is also clear that, as  $P_l$  decreases,  $(R_0)_c$  and  $a_c$  increase and that they reach saturated values for  $P_l = 10^{-5}$ .

From the first order solutions and using the method of iteration, we develop the higher order solutions that give  $R_1 = 0$ . Further, the vanishing of all the zero average non-linear terms from the first order solutions leads to  $w_1 = u_1 = T_1 = 0$ , and  $h_{01} = h_{10} = L_{01} = L_{10} = 0$  to satisfy (13). Therefore, from the third order equations we can write

$$L(W_2) = R_2 \nabla_1^2 W_0 + [(\overline{W_0 T_0})_m - \overline{W_0 T_0}] \nabla_1^2 W_0, \tag{18}$$

$$R_2 = \frac{a^2 + 1}{2a^2} \left[ \pi^2(a^2 + 1) + \frac{1}{P_l} \right] = \frac{R_0}{2(a^2 + 1)}. \tag{19}$$

In (18),  $L$  is a certain linear differential operator involving the Prandtl number  $Pr = \nu/\kappa^*$  and the dimensionless heat capacity  $M = (\rho c)^*/(\rho c)_f$ ; an overbar denotes the average over a horizontal plane, and the subscript 'm' denotes the average over a vertical line. Since  $R_2$  is always positive, subcritical solutions [22] are not possible in the present problem. In other words, the steady solution with finite amplitude is stable and the bifurcation of conduction into convection is super-critical rather than two sided.

The Nusselt number,  $Nu$ , following [22] is

$$Nu = \left[ 1 + \frac{2(R - R_0)}{R} \right]. \tag{20}$$

The ratio  $\frac{R Nu}{R_0 Nu_0} = \frac{H(R)}{H(R_0)}$ , where  $Nu_0$  is the value of  $Nu$  at  $R = R_0$ , is plotted in Figure 1 against  $R/R_0$  for  $M = 1$ ,  $Pr = 8$ , and  $P_l = 10^{-3}$  for various approximations, namely,  $R_2$ ,  $R_4$ ,  $R_6$ , and  $R_6$  (ZANL). From this figure, it is clear that  $R_6$  has brought the heat transport back very near to the  $R_2$ -curve in the range  $R_0 \leq R \leq 2.5R_0$ . One can anticipate that the  $R_6$ -curve, like the  $R_4$ -curve, will diverge to the right at some  $R$  greater than  $2.5R_0$  and the  $R_{10}$ -curve, like the

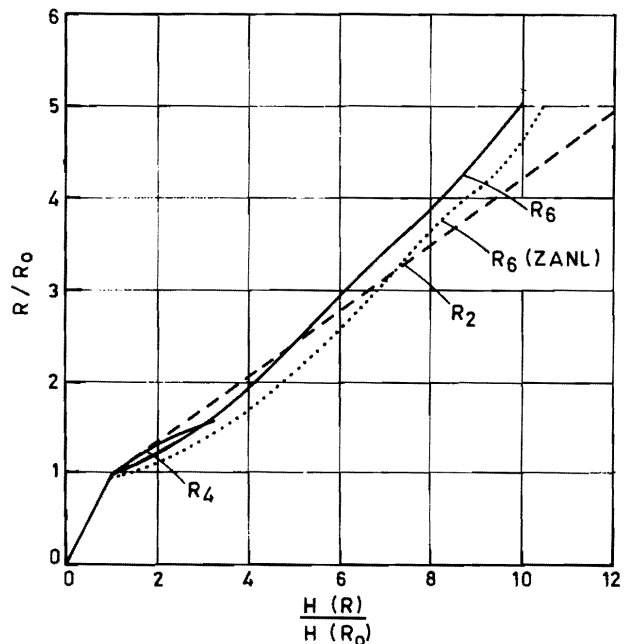


Figure 1. Heat Transport vs Rayleigh Number for Different Approximations for the Case  $M = 1$ ,  $Pr = 8$ , and  $P_l = 10^{-3}$

$R_6$ -curve, may be more nearly parallel to that for  $R_2$ . From this figure it is also clear that neglect of zero-average non-linear terms increases the amplitude of the predicted heat transport.

**3.2 Analysis for Three-Dimensional Motion with a Free Surface**

The power integral technique used in Section 3.1 is now extended to three-dimensional motion, with the object of determining the preferred cell pattern. Since the analysis is similar, only the results are presented and discussed. The linear solution analogous to (14)–(16) is  $W_0 = -(2\sqrt{2})\cos\pi lx \cos\pi my \sin\pi z$ , etc., where  $l^2 + m^2 = a^2$  and  $R_0$  is given again by (16).

To determine the first finite amplitude results,  $R_2$  is computed in a way similar to that for rolls and the influence of  $Pr$  is found even in the second order approximation itself. This  $R_2$ , as a function of  $Pr$ ,  $P_1$ , and  $l/m$ , has a triply infinite set of values. The ratio  $l/m$  cannot be chosen arbitrarily and has to be determined by the physics of the system. The question as to which of the infinite number of values of  $l/m$  is chosen by the fluid can be answered by considering the relative stability criterion [22].

By using this value of  $R_2$ , the heat transport  $\frac{(WT)_m}{2(R-R_0)}$  is computed for different values of  $Pr$  and  $P_1$ ; we find that the convective heat transport is maximum at  $l/m=0$  (that is, limiting rectangles) for  $Pr=0.1$ . As  $Pr$  increases to 0.45 and above, the occurrence of maximum convective heat transport crosses from  $l/m=0$  to  $l/m=1$ . By fixing  $Pr=0.1$  and changing  $P_1$ , from  $10^{-2}$  to  $10^{-3}$ , the occurrence of maximum convective heat transport changes from a limiting rectangle to a square. In particular, we note that for small values of  $P_1 (\leq 10^{-4})$  the convective heat transport is almost independent of  $Pr$ , a property exhibited by rolls. We also find that the limiting rectangle will convect maximum heat only when  $P_1^{-1} \leq 10^2$  and  $Pr=0.45$ . In all other cases, a square cell will convect more heat. In Figure 2,  $Nu$  is plotted against the filtration Rayleigh number  $R_L$  for different values of  $l/m$  with  $Pr=1$  and  $P_1=10^{-2}$ . We see that  $Nu$  increases with  $l/m$ . The results for the limiting rectangle can be obtained easily from the general rectangle and are compared with those for rolls. We find that the value of heat transport for the limiting rectangle differs markedly from that for rolls. In general, therefore, we conclude that rolls are preferred

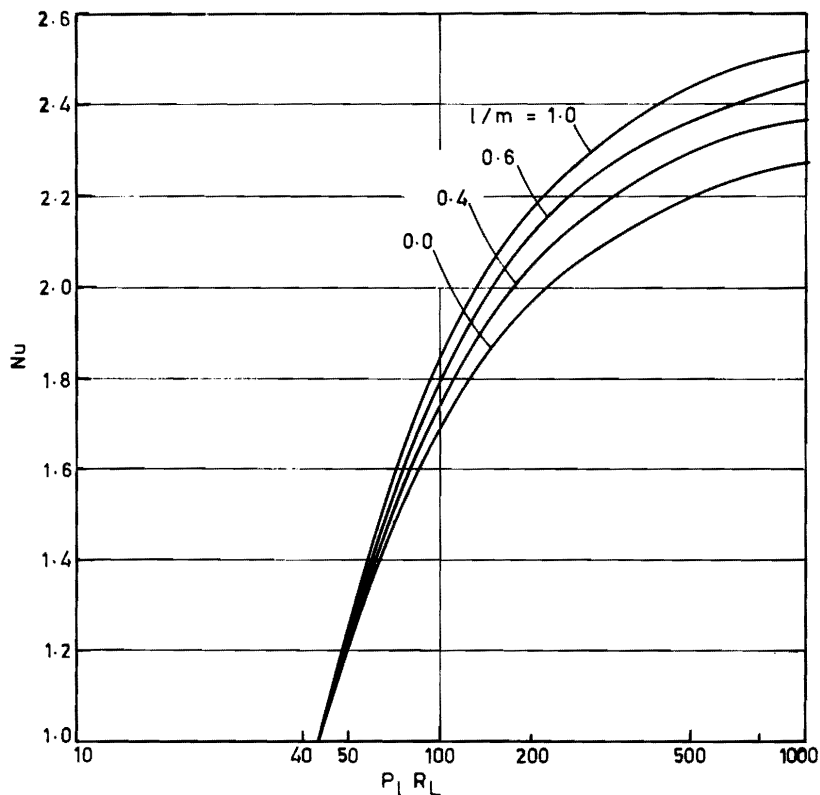


Figure 2. Heat Transport Curve for the Case of the General Rectangle with  $Pr=1.0$  for Different Values of  $l/m$

cells rather than squares and limiting rectangles because rolls transport more heat. However, if we consider only the three-dimensional motion, square cells are preferred to limiting rectangles. These conclusions are valid only when the viscosity is constant.

### 3.3 R<sup>2</sup> for Hexagons

The iterative procedure used in the previous sections is extended here to study hexagonal plan forms [22]. In this case we have

$$R_2 = \left[ \frac{1}{2} N_0 + \frac{\pi^2}{4} \left( T_{11} + \frac{T_{12}}{3} \right) \right] \quad (21)$$

$$T_{11} = \frac{3}{\pi^2 a^2} \left[ \frac{9}{2} (a^2 + 4) \times \left\{ \pi^2 (a^2 + 4) + \frac{1}{P_l} \right\} C_1 - \pi^2 Pr^{-1} (a^2 + 1) \right]$$

$$T_{12} = \frac{3}{\pi^2 (a^2 + 1)} \left[ \frac{9}{2} (3a^2 + 4) \times \left\{ \pi^2 (3a^2 + 4) + \frac{1}{P_l} \right\} C_2 - \pi^2 Pr^{-1} (a^2 + 1) \right].$$

The heat transport for a hexagonal plan form is computed using  $(WT)_m = \varepsilon^2 (W_0 T_0)_m$  and we find that it is smaller than that due to squares and greater than those due to limiting rectangles. Thus, square cells are the physically preferred cell patterns.

### 4. NON-LINEAR CONVECTION USING THE SPECTRAL METHOD

The power integral technique discussed in Section 3 to study the non-linear convection in a porous medium is based on a local non-linear analysis. In this analysis, to take care of secular and resonant terms, an orthogonalization process was built in. This results in the consideration of only even modes of interaction and remains silent about the cross-interaction of the terms of different modes. The spectral method, discussed in this section, overcomes this difficulty. We just explain the method briefly and try to cover some new results which were not dealt with in [41].

Introducing the stream function  $\psi$ , such that

$$u = -\frac{\partial \psi}{\partial Z}, \quad v = \frac{\partial \psi}{\partial x},$$

Equations (8)–(10) take the form

$$\left( \nabla^2 - \frac{1}{P_l} \right) \nabla^2 \psi + \frac{\partial T}{\partial x} = \frac{1}{Pr} B \quad (22)$$

$$\nabla^2 T + R \frac{\partial \psi}{\partial x} = H, \quad (23)$$

where  $T$  is a dimensionless temperature distribution, and  $B = \frac{\partial(\psi, \nabla^2 \psi)}{\partial(x, z)}$  and  $H = \frac{\partial(\psi, T)}{\partial(x, z)}$  are the momentum and thermal advection Jacobians. We note that, in all the dimensionless parameters,  $\pi$  appears because of our choice of the length scale, namely,  $d/\pi$ . The present  $P_l$  is  $\pi^2$  times the  $P_l$  used in Section 3. Since we assume stress free boundaries, we have

$$\psi = \nabla^2 \psi = T = 0 \text{ at } z = 0, 1. \quad (24)$$

We consider the spectral representation

$$\psi = \sum_{\gamma} \psi_{\gamma} S_{\gamma}, \quad S_{\gamma} = -\exp\{i(lax + nz)\} \quad (25)$$

$$T = \sum_{\gamma} T_{\gamma} C_{\gamma}, \quad C_{\gamma} = i \exp\{i(lax + nz)\}, \quad (26)$$

where  $a$  is the horizontal wave number of the first mode,  $\Sigma$  means summation over all integral lattice points in the  $l, n$ -plane, and  $\gamma$  is a vector with components  $(l, n)$ . The representations (25) and (26) transform (22) and (23) into the spectral domain with the orthogonal property:

$$\int_s S_{\beta}^* S_{\alpha} dS = \int_s C_{\beta}^* C_{\alpha} dS = \delta_{\beta, \alpha}, \quad (27)$$

where  $S$  is the surface  $0 \leq x \leq 2\pi/a$ ,  $-\pi < z < \pi$ ,  $dS$  is the elementary area divided by the total area  $4\pi^2/a$  of the region, and  $S_{\beta}^*$  and  $C_{\beta}^*$  are the complex conjugates of  $S_{\beta}$  and  $C_{\beta}$ . Equations (12) and (13), using (15) and (16), become

$$T_{\gamma} = \frac{H_{\gamma}}{n^2}, \quad \text{for } l=0 \quad (28)$$

$$\alpha_{\gamma}^2 T_{\gamma} - laR \psi_{\gamma} = -aH_{\gamma}$$

$$(\alpha_{\gamma}^4 + \alpha_{\gamma}^2/P_l) \psi_{\gamma} = aT_{\gamma} - \frac{a}{Pr} B_{\gamma} \text{ for } l \neq 0 \quad (29)$$

where

$$\alpha_{\gamma}^2 = l^2 a^2 + n^2$$

$$B_{\gamma} = -\sum_{\gamma_1} \sum_{\gamma_2} (l_1 n_2 - l_2 n_1) \alpha_{\gamma_1}^2 \psi_{\gamma_1} \psi_{\gamma_2} \quad (30)$$

$$H_\gamma = \sum_{\gamma_1} \sum_{\gamma_2} (l_1 n_2 - l_2 n_1) \psi_{\gamma_1} T_{\gamma_2} \quad (31)$$

and the pairs  $\gamma_1 + \gamma_2$  satisfy the selection rule

$$\gamma = \gamma_1 + \gamma_2, \text{ that is, } l = l_1 + l_2, n = n_1 + n_2. \quad (32)$$

#### 4.1 Modal Rayleigh Number

Elimination of  $T_\gamma$  in (29) leads to

$$(R - R_\gamma) \psi_\gamma = \frac{1}{l} H_\gamma + \frac{\alpha_\gamma^2}{a l^2 Pr} B_\gamma \quad (33)$$

where

$$R = \alpha^2 / l^2 a^2 + \alpha_\gamma^4 / l^2 a^2 P_l \quad (34)$$

is called the modal Rayleigh number for a given mode  $\gamma = (l, n)$ .  $R$  is a continuous function of  $a^2$  and, in fact, is a hyperbolic profile. The critical  $R_\gamma$ , denoted by  $(R_\gamma)_c$ , and the critical wave number  $a_c$  are given by

$$(R_\gamma)_c = \frac{1}{32n^2} \left[ 3n^2 - \frac{1}{P_l} + \sqrt{(n^2 + 1/P_l)(9n^2 + 1/P_l)} \times \right. \\ \left. [3n^2 + 1/P_l + (n^2 + 1/P_l)(9n^2 + 1/P_l)] \right] \quad (35)$$

$$a_c^2 = \frac{1}{4l^2} \left[ -(n^2 + 1/P_l) + \sqrt{(n^2 + 1/P_l)(9n^2 + 1/P_l)} \right]. \quad (36)$$

These are true for any mode consistent with the selection rule [41]. The minimum critical  $R_\gamma$  and  $a_c$  are obtained for the fundamental mode (1, 1) in the form

$$(R_{11})_c = \frac{1}{32} \left[ 3 - \frac{1}{P_l} + \sqrt{\left(1 + \frac{1}{P_l}\right)\left(9 + \frac{1}{P_l}\right)} \right] \times \\ \left[ 3 - \frac{1}{P_l} + \sqrt{\left(1 + \frac{1}{P_l}\right)\left(9 + \frac{1}{P_l}\right)} \right] \quad (37)$$

$$a_c^2 = \frac{1}{4} \left[ -1 - \frac{1}{P_l} + \sqrt{\left(1 + \frac{1}{P_l}\right)\left(9 + \frac{1}{P_l}\right)} \right]. \quad (38)$$

These are computed for different values of  $P_l$  and the results are shown in Table 2.

**Table 2. Critical Modal Rayleigh Numbers and Wave Numbers for the Fundamental Mode**

$P_l$	$a_c$	$(R_{11})_c$	$(R_{11})_c P_l$
$\infty$	0.5	$6.75 \times 10^0$	—
$10^{-2}$	0.9303	$4.824 \times 10^1$	4.761219
$10^{-3}$	0.9905	$4.133 \times 10^2$	4.078581
$10^{-4}$	0.9990	$4.061 \times 10^3$	4.007891
$10^{-5}$	0.9996	$4.054 \times 10^4$	4.000789

We note that when  $P_l \rightarrow \infty$ , the results coincide with [46] for viscous flow; for  $P_l = 10^{-5}$  they tend to the LD model [22]. Note that their  $R_c$  differs from our  $R_c$  by a factor  $\pi^4$  because of our choice of the length scale. For small values of  $P_l (< 10^{-3})$ , the values of  $(R_{11})_c / P_l$  and  $a_c$  tend toward those given by Lapwood [7].

The variation of  $R_\gamma$  against  $a^2$ , for different modes  $\gamma$ , is computed and the results are shown in Figure 3. This figure depicts the interaction of different modes for different values of  $P_l$ .

Rudraiah and Balachandra Rao [41] have introduced  $\exp\{i(lax + nz)\}$  instead of the apparently more natural  $\exp\{i(bx + nz)\}$ . The reason for this complication is the implied presence of side walls that limit  $b$  to integral multiples of a basic minimum  $b (= a, \text{ say})$ . Thus  $b = la$ , where  $a$  is fixed and  $l = 1, 2, 3, \dots$ . It is clearest to refer calculations such as  $(R_\gamma)_c$  to  $b$ . For each value of  $n$ , the curve  $(R_\gamma)_c$  is as indicated in Figure 4 for different values of  $P_l$ . If the side walls are nearer to each other, the smallest value of  $b = a$  lies to the right of the minimum  $b_c$  of  $(R_\gamma)_c$ , so that, if  $(R_\gamma)_c$  is increased adiabatically from zero, critical conditions are reached first at  $b = a$ , corresponding to the onset of one convection cell that fills the box. If the side walls are far from each other the smallest value of  $b (= a)$  lies to the left of  $b_c$ ; indeed, for a large 'box', considered here, it may be so far to the left that  $a, 2a, 3a$  all lie to the left of  $b_c$ . Now, as  $(R_\gamma)_c$  is increased adiabatically from zero, critical conditions are reached first for some integral multiple,  $la$  say, of the basic periodicity, corresponding to the onset of convective motion with many cells in the box depending on the value of  $l$ . Physically this implies that the larger the box, the smaller the  $a$ , and that more cells can be fitted into the box. In the limit of an infinitely large box ( $a \rightarrow 0$ ), the spacing of modes in the figure tends to zero, and we recover a full stability curve. In a physical system, however, there are only  $l$  cells and, for odd  $l$ , there is one more cell turning in one direction than in the other. Because of the prominence given to the study of finite amplitude convection of odd parity, the even parity modes  $\gamma = (2, 1), (4, 1) \dots$  are excluded from Figure 3. In this sense, the discussion of the linear stability problem from Figure 3 in [41] is incomplete. Therefore, in Figure 4 we have taken the even parity terms. If the separation of the vertical walls  $D$  of the box is small enough, the  $\gamma = (1, 1)$  mode enters first when  $R_2$  is adiabatically increased from zero as shown in Figure 4. However, if  $D$  is adiabatically increased, a stage will be reached when the  $\gamma = (2, 1)$  mode has a smaller  $(R_\gamma)_c$  as shown in Figure 4. In that

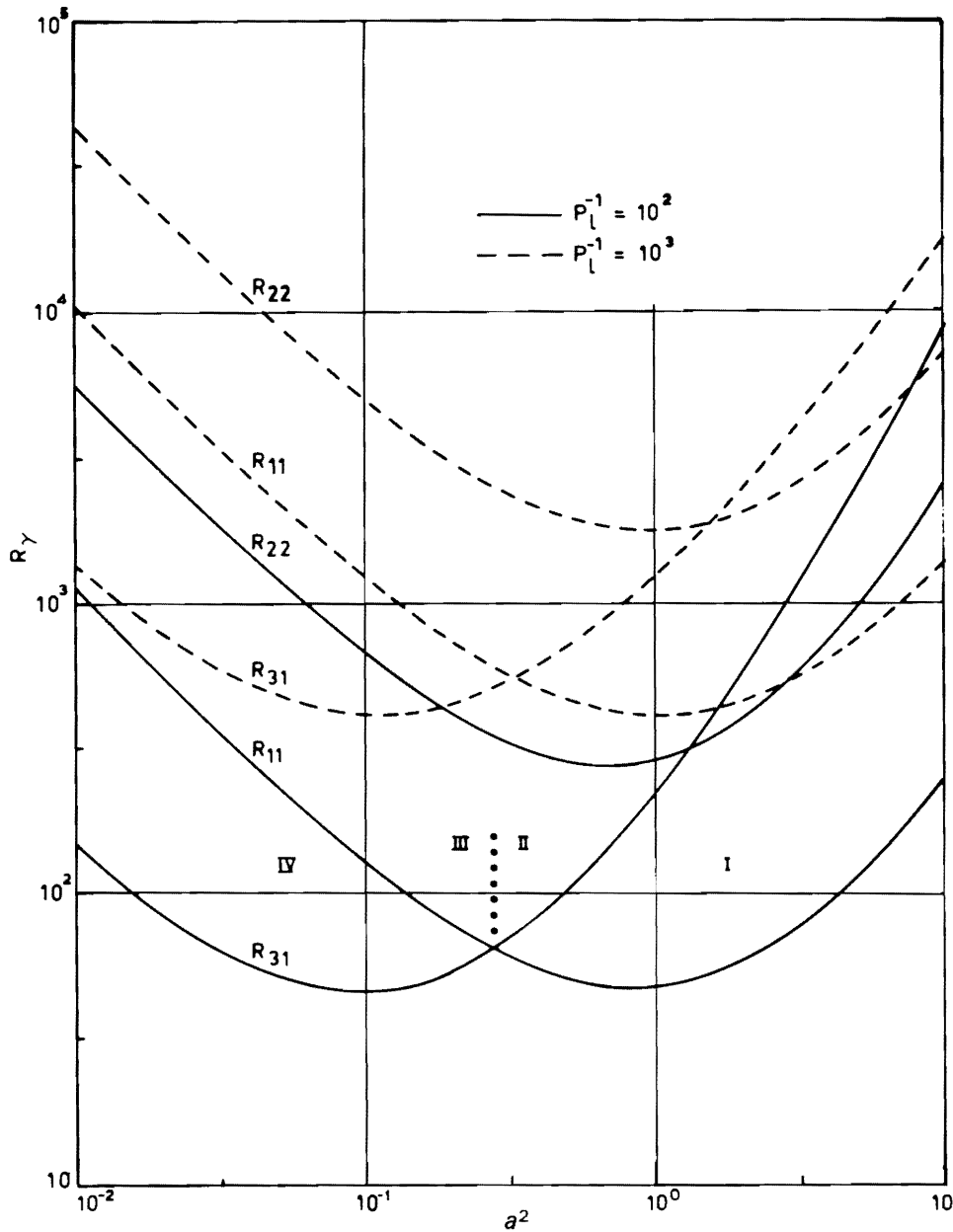


Figure 3. Modal Rayleigh Number  $R_\gamma$  as a Function of  $a^2$

case when convection first occurs it will be as a two cell pattern. By considering odd parity modes in Figure 3, they [41] have ruled out this possibility. We note that since the finite amplitude solution is based on the linear stability problem, it can describe the stability of the system only in the range in which the fluid is not unstable to other disturbances. Therefore, one has to consider either odd parity or even parity modes. In this paper, to study finite amplitude convection we consider only odd parity modes.

#### 4.2 Method of Solution of the Spectral Equation

The contribution of the non-linear advection terms for the onset of convection is considered in this section. For this, we expand  $\psi_\gamma$  in (33) in the form

$$\psi_\gamma = \psi_{\gamma,r} \Delta^r + \psi_{\gamma,r+1} \Delta^{r+1} + \dots \quad (39)$$

Here,

$$\Delta = \sqrt{R - (R_{11})_c}$$

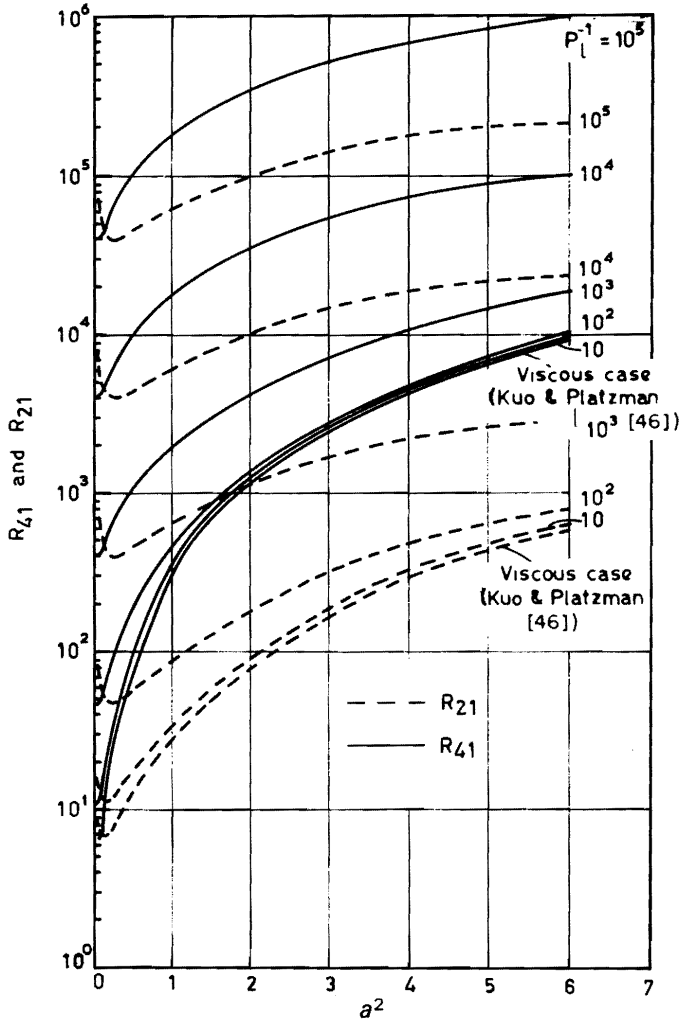


Figure 4. Modal Rayleigh Number vs  $a^2$  for Even Modes

and  $r$  is the order or magnitude of an element  $\psi_{\gamma}$ , being the lowest power of  $\Delta$  in the expansion. For example, since  $\psi_{11}$  is, by definition, a first order element we can expand it in the form

$$\psi_{11} = \psi_{111}\Delta + \psi_{113}\Delta^3 + \dots \quad (40)$$

Then (33), using (39) and equating the coefficients of  $\Delta^r$ , takes the form

$$(R_{\gamma} - R_{11})\psi_{\gamma,r} = \psi_{\gamma,r-2} + \frac{1}{l}H_{\gamma,r} + \frac{\alpha_{\gamma}^2}{alPr}B_{\gamma} \quad (41)$$

The spectral coefficients  $\psi_{111}$ ,  $\psi_{113}$ ,  $\psi_{133}$ ,  $\psi_{224}$ , and  $\psi_{244}$  evaluated at  $a = a_c$  for different values of  $P_l$  and  $Pr$  are shown in Table 3. The table confirms the following.

- (i) The values of  $\psi_{111}$  and  $\psi_{113}$ , both of which contribute to  $\psi_{11}$ , decrease with decreasing  $P_l$  but are independent of  $Pr$ . A comparison of these

with those of the LD model [22] reveals that  $\psi_{111}$  differs from that of the LD model whereas  $\psi_{113}$  has the same qualitative behavior in the two models.

- (ii)  $\psi_{133}$ , which contributes to the  $\gamma = (1, 3)$  mode, also decreases with decreasing  $P_l$  and is also independent of  $Pr$ .
- (iii)  $\psi_{224}$  and  $\psi_{244}$  decrease numerically with decreasing  $P_l$  and increasing  $Pr$ .
- (iv) In general, the effect of  $P_l$  is to decrease the spectral elements for a given  $Pr$ , thus damping the convective system.

### 4.3 Spectral Representation of the Heat Transport

The Nusselt number in this case takes the form

$$Nu = 1 - \frac{1}{R} \sum_{\gamma} n_{\gamma} T_{\gamma} \quad (42)$$

where  $\gamma = (0, n_{\gamma})$  and  $n_{\gamma}$  ranges over positive and negative integers. We expand the spectral element in (42) in powers of the parameter  $\Delta$  in the form

$$\bar{T}_{02} = \bar{T}_{022}\Delta^2 + \bar{T}_{024}\Delta^4 + \bar{T}_{026}\Delta^6 + \dots$$

$$\bar{T}_{04} = \bar{T}_{044}\Delta^4 + \bar{T}_{046}\Delta^6 + \dots,$$

where  $\bar{T}_{0np}$  is a constant, being the coefficient of  $\Delta^p$  in the power series expansion of the mean temperature spectral element  $\bar{T}_{0n}$ . Since  $\bar{T}_{\gamma}$  appear in even powers of  $\Delta$ , it is more convenient to use a new parameter  $\varepsilon$  defined by

$$\varepsilon = \frac{\Delta^2}{R_{11}} = \frac{R - R_{11}}{R_{11}}$$

so that  $R = (1 + \varepsilon)R_{11}$ .

Now,

$$Nu = a_0 + a_2\varepsilon + a_4\varepsilon^2 + \dots,$$

where

$$a_0 = 1, \quad a_2 = -4\bar{T}_{022},$$

$$a_4 = -a_2 - 4R_{11}(\bar{T}_{024} + 2\bar{T}_{044}),$$

$$\bar{T}_{022} = -\frac{1}{2}, \quad \bar{T}_{024} = -\frac{a^2}{16A},$$

$$\bar{T}_{044} = -\frac{a^2(a^4 + 10a^2 + 41)}{16(a^2 + 1)^2 A},$$

$$A = 91 + \frac{10}{P_l} + 2(15 + 1/P_l)a^2 + 3a^4.$$

Then

$$Nu^{(0)} = a_0 = 1, \quad Nu^{(2)} = a_0 + a_2\varepsilon,$$

$$Nu^{(4)} = a_0 + a_2\varepsilon + a_4\varepsilon^2.$$

**Table 3. Values of Spectral Coefficients for Different Values of  $P_l$  and  $Pr$**

$P_l$ and ( $a_c$ )	$Pr$	$\psi_{111}$	$\psi_{113}$	$\psi_{133}$	$\psi_{224}$	$\psi_{244}$
$10^{-2}$ (0.865)	0.025	$3.791 \times 10^{-1}$	$2.581 \times 10^{-3}$	$1.722 \times 10^{-4}$	$7.700 \times 10^{-4}$	$-7.058 \times 10^{-5}$
	0.687	$3.791 \times 10^{-1}$	$2.581 \times 10^{-3}$	$1.722 \times 10^{-4}$	$8.210 \times 10^{-5}$	$-4.558 \times 10^{-6}$
	8.0	$3.791 \times 10^{-1}$	$2.581 \times 10^{-3}$	$1.722 \times 10^{-5}$	$5.835 \times 10^{-5}$	$-2.279 \times 10^{-6}$
	$\infty$	$3.791 \times 10^{-1}$	$2.581 \times 10^{-3}$	$1.722 \times 10^{-5}$	$5.612 \times 10^{-5}$	$-2.065 \times 10^{-6}$
$10^{-3}$ (0.981)	0.025	$3.569 \times 10^{-1}$	$4.488 \times 10^{-4}$	$3.278 \times 10^{-5}$	$2.413 \times 10^{-5}$	$-3.273 \times 10^{-6}$
	0.687	$3.569 \times 10^{-1}$	$4.488 \times 10^{-4}$	$3.328 \times 10^{-5}$	$2.510 \times 10^{-6}$	$-2.110 \times 10^{-7}$
	8.0	$5.569 \times 10^{-1}$	$4.488 \times 10^{-4}$	$3.278 \times 10^{-5}$	$1.764 \times 10^{-6}$	$-2.053 \times 10^{-7}$
	$\infty$	$3.569 \times 10^{-1}$	$4.488 \times 10^{-4}$	$3.278 \times 10^{-5}$	$1.694 \times 10^{-6}$	$-9.538 \times 10^{-8}$
$10^{-4}$ (0.998)	0.025	$3.539 \times 10^{-1}$	$4.861 \times 10^{-5}$	$3.596 \times 10^{-6}$	$3.524 \times 10^{-8}$	$-4.127 \times 10^{-11}$
	0.687	$3.539 \times 10^{-1}$	$4.861 \times 10^{-5}$	$3.596 \times 10^{-6}$	$3.653 \times 10^{-9}$	$-2.66 \times 10^{-12}$
	8.0	$3.539 \times 10^{-1}$	$4.861 \times 10^{-5}$	$3.596 \times 10^{-6}$	$2.563 \times 10^{-9}$	$-1.327 \times 10^{-12}$
	$\infty$	$3.539 \times 10^{-1}$	$4.861 \times 10^{-5}$	$3.596 \times 10^{-6}$	$2.460 \times 10^{-9}$	$-1.202 \times 10^{-12}$

The variation of  $Nu$  with  $a^2$  is shown in Figure 5. We see that the heat transport is less than that in the LD model. The second order  $Nu$  is given by

$$Nu^{(2)} = 1 + 2\epsilon = \frac{2Ra^2}{(2a^2 + 1)^2(a^2 + 1 + 1/P_l)} - 1. \quad (43)$$

Figure 5 presents  $Nu$  computed for  $R=1.6R_c$  and  $2R_c$  and for different values of  $P_l$ . In this figure, for the sake of comparison, the LD model and pure viscous

flow results are also shown. We see that, in the DLB model discussed here, the maximum value of  $Nu^{(2)}$  varies with  $P_l$ , whereas in the LD model and in pure viscous flow it is independent of  $P_l$  because  $a_c$  is independent of  $P_l$ . We also see that for small values of  $P_l$  the results of the DLB model tend to those of the LD model whereas for large values of  $P_l$  they tend to pure viscous flow. This proves that the results of the DLB model are more general and the other two cases can be obtained with a proper limiting process.

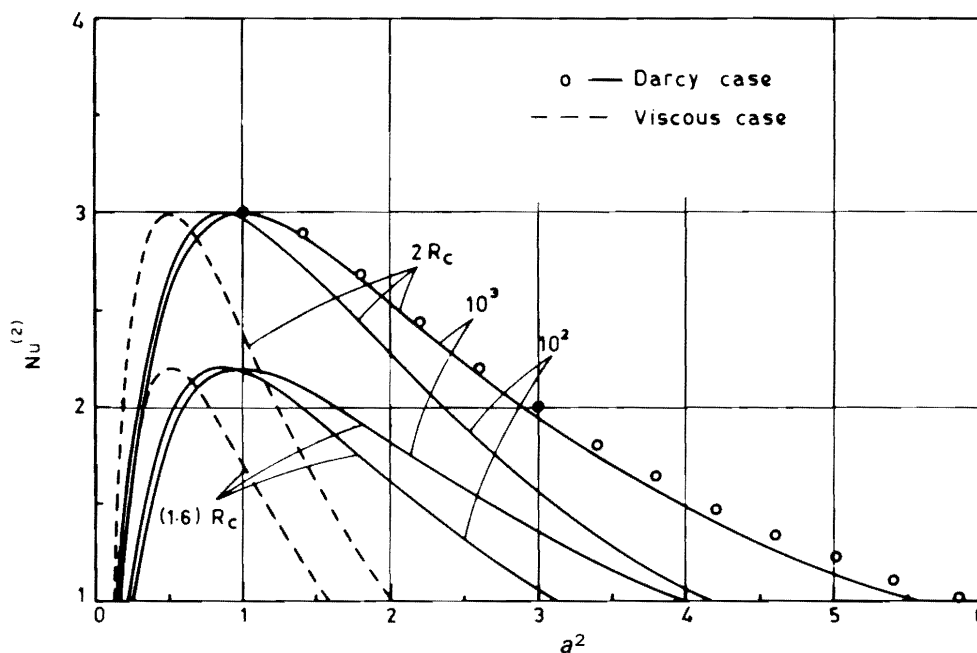


Figure 5. Variation of  $Nu^{(2)}$  with  $a^2$  for  $R=1.6R_c, 2R_c$

### 5. NUMERICAL MODEL USING THE GALERKIN TECHNIQUE

The non-linear convection discussed in the previous sections based on analytical procedures is restricted to finite amplitudes. In other words, the results are valid only for restricted values of  $R - R_c$ .

We develop in this section, following Friedrich and Rudraiah [24,47], a numerical model based on the Galerkin technique to discuss large amplitude convection in a coarse porous layer of finite thickness, but of infinite horizontal extent. We consider only two-dimensional motion. In the Galerkin technique used here, the stream function and temperature are developed in the form:

$$\begin{aligned} \psi &= \sum_{m=1}^M \sum_{n=1}^N a_{mn} \sin m\pi a_c x \sin n\pi z \\ T &= \sum_{m=1}^M \sum_{n=1}^N b_{mn} \cos m\pi a_c x \sin n\pi z \end{aligned} \tag{44}$$

which satisfy the conditions (24) and symmetry conditions

$$\frac{\partial^2 \psi}{\partial x^2} = 0, \frac{\partial T}{\partial x} = 0 \text{ on } x=0, n/a \text{ (} n=1, 2, \dots \text{)}. \tag{45}$$

These conditions are all verified by the trial function (44). In the Galerkin technique, the residual is formed by means of the trial functions and we integrate over the whole volume. From (8) to (11), the set of ordinary differential equations for the amplitudes  $a_{mn}$  and  $b_{mn}$  of the harmonic components is derived under the assumption of two-dimensional motion:

$$\begin{aligned} \frac{da_{pq}}{dt} &= -Pr\pi^2(p^2 a^2 + q^2)a_{pq} - \frac{PrR_{ap}}{\pi(p^2 a^2 + q^2)}b_{pq} - \frac{Pr}{P_l}a_{pq} \\ &+ \frac{\pi^2 a}{4(p^2 a^2 + q^2)} \sum_{m=1}^{p-1} \sum_{n=1}^{q-1} (mq - np)[(p-m)^2 a^2 \\ &+ (q-n)^2]a_{mn}a_{p-m, q-n} \\ &+ \sum_{m=p+1}^M \sum_{n=q+1}^N (mq - np)[(p-m)^2 a^2 + (q-n)^2 \\ &- (m^2 a^2 + n^2)]a_{n-p, n-q}a_{mn} \\ &+ \sum_{m=p+1}^M \sum_{n=1}^{q-1} [p(n-q) + mq][m^2 a^2 \\ &+ (q-n)^2]a_{m-p, n}a_{m, q-n} \\ &+ \sum_{m=p+1}^M \sum_{n=q+1}^N [q(m-p) + np][(m-p)^2 a^2 + n^2 \\ &- m^2 a^2 + (n-q)^2]a_{m, n-q}, a_{m-p, n} + \end{aligned}$$

$$\begin{aligned} &+ \sum_{m=p+1}^M \sum_{n=1}^N (np - mq) \times \\ &[(m-p)^2 a^2 + (q-n)^2]a_{mn}a_{m-p, q-n} \\ &+ \sum_{m=1}^{p-1} \sum_{n=q+1}^N [p(q-n) - mq] \times \\ &[(p-m)^2 a^2 + n^2]a_{m, n-q}a_{p-m, n} \\ &+ \sum_{m=1}^{p-1} \sum_{n=q+1}^N (np - mq) \times \\ &[(p-m)^2 a^2 + (n-q)^2]a_{mn}a_{p-m, n-q} \\ &(1 \leq p \leq M, 1 \leq q \leq N), \end{aligned} \tag{46}$$

$$\begin{aligned} \frac{db_{pq}}{dt} &= -\pi^2(p^2 a^2 + q^2)b_{pq} - \pi a p a_{pq} \\ &+ \left(1 - \frac{1}{2}\delta_{p0}\right) \frac{\pi^2 a}{4} \sum_{m=0}^{p-1} \sum_{n=1}^{q-1} (np - mq)a_{p-m, q-n}b_{mn} \\ &+ \sum_{m=p}^M \sum_{n=q+1}^N (np - mq)a_{mn}b_{m-p, n-q} \\ &+ \sum_{m=p+1}^M \sum_{n=q+1}^N [p(q-n) - mq]a_{m-p, n}b_{m, n-q} \\ &+ \sum_{m=p}^M \sum_{n=q+1}^N [p(q-n) - mq]a_{m, n-q}b_{m-p, n} \\ &+ \sum_{m=p+1}^M \sum_{n=q+1}^N (np - mq)a_{m-p, n-q}b_{mn} \\ &+ \sum_{m=0}^{p-1} \sum_{n=q+1}^N [p(n-q) + mq]a_{p-m, n}b_{m, n-q} \\ &+ \sum_{m=0}^{p-1} \sum_{n=q+1}^N (mq - np)q_{p-m, n-q}b_{mn} \\ &+ \sum_{m=1}^M \sum_{n=1}^N [q(m-p) + np]a_{m, q-n}b_{m-p, n} \\ &+ \sum_{m=p+1}^M \sum_{n=1}^{q-1} (mq - np)a_{m-p, q-n}b_{mn} \\ &(0 \leq p \leq M, 1 \leq q \leq N). \end{aligned} \tag{47}$$

We truncate the sums and calculate the systems with a maximum number of modes  $k = M + N$  not larger than 12. The non-linear terms in (46) have not been written explicitly for want of space but are included in the computation.

#### 5.1 Numerical Procedure

Because of the excessive length of (46) and (47) for  $k > 3$ , a special FORTRAN routine has been written

with the purpose of generating the right-hand sides in a form most suitable for rapid integration. The analytical solutions discussed in the earlier sections provide a set of initial conditions for the coefficients. Three different integration codes are used: (i) the first code ODE [48] uses a modified divided difference form of the Adams-PECE formulas and local extrapolation, in order to improve absolute stability and accuracy. These formulas consist of an Adams-Bashforth predictor of order  $k$  and an Adams-Moulton correction of order  $k+1$ . The code controls the local error per unit step; (ii) the second code, RKF45, uses Fehlberg's fourth-fifth order Runge-Kutta method; (iii) the third code, RKF48, is an adaptation of the implementation of Fehlberg's fourth-fifth order Runge-Kutta method to more accurate seventh-eighth order Fehlberg's formulas. All three codes allow for the specification of relative and absolute error tolerances for error tests and choose their own integration steps. The required critical wave number is found from solving the sixth order polynomial (17) numerically. While searching for steady state solutions we find that certain representations and too high Rayleigh numbers produce chaotic solutions. The effect of viscous force on their appearance is worked out. Table 4 compares the  $Nu$  obtained from different codes.

**Table 4. Comparison of Three Codes for  $P_l = 10^{-3}$ ,  $R/R_c = 6$ , and  $Pr = 6.8$  (Water)**

	ODE	RKF45	RKF48
$Nu$	3.980122	3.980122	3.780122
CP seconds	42.4	46.6	107.0
Number of steps	5	5	5

The three codes converge towards the same  $Nu$ , with the same number of integration steps, when successive  $Nu$  differ by less than  $10^{-6}$ . Then, a steady state of the solution was defined through the criterion:

$$|Nu(t + \Delta t) - Nu(t)| < 10^{-6}$$

In terms of the coefficients,  $Nu$  takes the form

$$Nu = 1 - \pi \sum_{n=1}^N nb_{0n}$$

Since the code ODE turned out to be most effective to solve such problems, it has been used during all further calculations. We have varied the maximum number of modes in Figure 6 in order to find out how well different  $k$  represent reality. For  $k=6$  and 8,

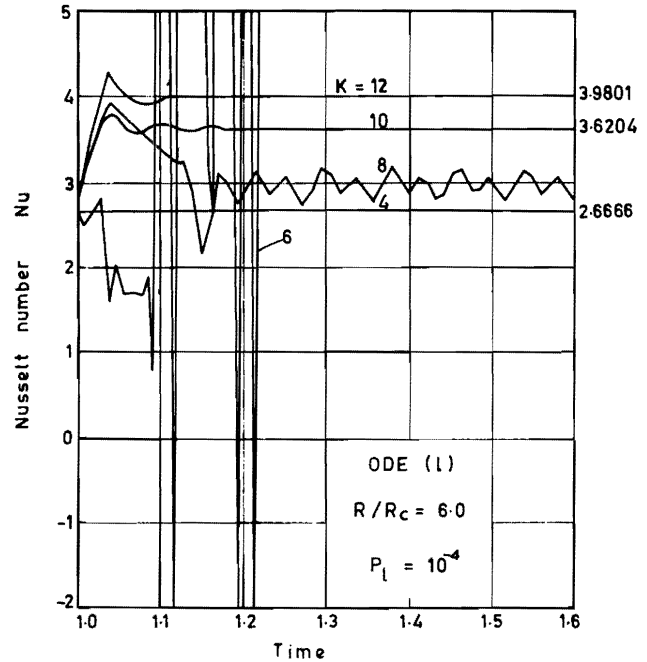


Figure 6.  $Nu$  Depends on the Size of the Representation; Certain Modes Produce Chaotic Solutions

solutions exhibited a random behavior, whereas they behaved well for  $k=10$  and 12. An alternative way of producing chaotic solutions is to choose Rayleigh numbers larger than  $6R_c$ . Figure 7, illustrates this effect for a system of order 120 ( $k=12$ ) at  $R=10R_c$ .

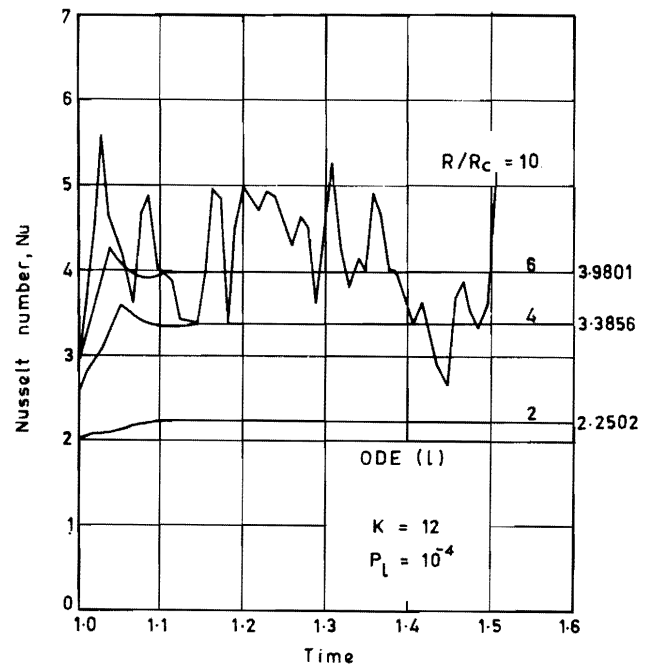


Figure 7. Chaotic Solutions as a Result of Too High Rayleigh Numbers

The streamline and isotherm patterns obtained from the numerical technique are in close agreement with the analytical results obtained in the previous sections. Further, we are able to recover the special cases of purely viscous flow and a purely densely packed porous medium of the LD model, both of which have been studied in the literature. We note that further extensive studies are necessary to find stable and unstable critical points for large representations.

## 6. CONCLUSIONS

Analytical and numerical procedures are used to study non-linear convection in a porous medium of porosity close to unity with convective acceleration and viscous force. The analytical procedure is based on the power integral technique (hereafter called PIT) and the spectral analysis technique (SAT). We find that PIT is useful to study the detailed cell pattern and the effect of Prandtl number on convection, but it is silent about the cross-interactions of the different modes. SAT overcomes this deficiency through the modal Rayleigh number. Further, SAT predicts the possibility of the existence of a steady solution with two self-excited modes in certain regions and the existence of convection as a two-cell pattern, which could not be brought out from PIT. Another important difference between the two techniques is the evaluation of the averaged temperature profile. Although these techniques are used in this paper under the assumption of small  $R - R_c$ , that is, small temperature gradients, the SAT can also be used for large values of  $R - R_c$  by expanding the spectral coefficients using a suitable parameter [49],  $(R - R_c/R)^{1/2}$ , say. This is not possible in PIT. The effect of permeability, in both the techniques, is to contract the cells and to inhibit the onset of convection. This effect is analogous to that of a magnetic field on convection [50] in magnetohydrodynamics.

The numerical techniques, ODE, RKF45, and RKF48, employed in this paper take care of large amplitudes, that is, large values of  $R - R_c$ . We find that our analytical results are in close agreement with the numerical data for small values of  $R - R_c$ . In particular, it is shown that certain representations and too high Rayleigh numbers produce chaotic solutions.

## ACKNOWLEDGMENT

This work was supported by the UGC under the DSA program. The numerical work reported in this

paper was supported by the Department of Science and Technology, grant No. HCS/DST/1114/81.

The author is grateful to Professor Dr. R. Friedrich, Institute for Fluid Mechanics, Technical University of Munich, for his help on numerical procedure.

## REFERENCES

- [1] J. P. Caltagirone, 'Convection in a Porous Medium', in *Convective Transport and Instability Phenomena*, eds. J. Ziener and H. Oertel, Jr. West Germany; Braun, 1982, p. 199.
- [2] H. Darcy, *Les Fontaines Publiques de la Ville de Dijon*, Paris: V. Dalmont, 1856.
- [3] H. S. Hele-Shaw, 'The Flow of Water', *Nature*, **58** (1898), p. 315.
- [4] H. Lamb, *Hydrodynamics*, 6th edition. New York: Dover, 1975.
- [5] J. Bear, *Dynamics of Fluids in Porous Media*. New York: American Elsevier, 1972.
- [6] C. W. Horton and F. T. Rogers, Jr., 'Convection Currents in a Porous Medium', *Journal of Applied Physics*, **16** (1945), p. 369.
- [7] E. R. Lapwood, 'Convection of a Fluid in a Porous Medium', *Proceedings of the Cambridge Philosophical Society*, **44** (1948), p. 508.
- [8] Y. Katto and T. Masuoka, 'Criterion for the Onset of Convective Flow in a Fluid in a Porous Medium', *International Journal of Heat Mass Transfer*, **10** (1967), p. 297.
- [9] J. W. Elder, 'Steady Free Convection in a Porous Medium Heated from Below', *Journal of Fluid Mechanics*, **27** (1967a), p. 29.
- [10] J. W. Elder, 'Transient Convection in a Porous Medium', *Journal of Fluid Mechanics*, **27** (1979b), p. 609.
- [11] M. Combarrous and S. Bories, 'Modelisation de la Convection Naturelle on Sein d'une Couche Poreuse Horizontale—Laide d'un Coefficient de Transfert Solide—Fluide', *International Journal of Heat and Mass Transfer*, **17** (1974), p. 505.
- [12] B. K. Hartline and C. R. B. Lister, 'Thermal Convection in a Hele-Shaw Cell', *Journal of Fluid Mechanics*, **79** (1977), p. 379.
- [13] B. K. Hartline and C. R. B. Lister, 'An Experiment to Verify the Permeability of Hele-Shaw Cells', *Geophysics Research Letters*, **5** (1978), p. 225.
- [14] G. Hamel, 'Uber Ground Water Stromung', *Zeitschrift für Angewandte Mathematik und Mechanik*, **14** (1934) p. 129.
- [15] C. S. Yih, *Dynamics of Nonhomogeneous Fluids*. New York: Macmillan, 1965, p. 197.
- [16] P. A. C. Raats, 'The Role of Inertia on the Hydrodynamics of Porous Media', *Archives of Rational Mechanical Analysis*, **44** (1972), p. 267.
- [17] K. Yamamoto and Z. Yoshida, 'Flow Through a Porous Wall with Convective Acceleration', *Journal of the Physical Society of Japan*, **37** (1974), p. 774.
- [18] D. R. Westbrook, 'Stability of Convective Flow in a Porous Medium', *Physics of Fluids*, **12** (1969), p. 1547.
- [19] R. P. Prabhmani and N. Rudraiah, 'Thermal Diffusion and Convective Stability of a Two Component Fluid in a Porous Medium', *Proceedings*

- of the 5th International Heat Transfer Conference, Tokyo, Japan CT3.1 (1974), p. 79.
- [20] R. P. Prabhmani and N. Rudraiah, 'Linear Convective Stability and Thermal Diffusion of a Horizontal Quiescent Layer of a Two Component Fluid in a Porous Medium', *International Journal of Engineering Science*, **18** (1980), p. 1565.
- [21] D. D. Joseph, 'Stability of Fluid Motions, II', *Springer Tracts on Natural Philosophy*, 1976.
- [22] N. Rudraiah and P. K. Srimani, 'Finite Amplitude Cellular Convection in a Fluid Saturated Porous Layer', *Proceedings of the Royal Society of London*, **A373** (1980), p. 199.
- [23] N. Rudraiah and S. Balachandra Rao, 'Nonlinear Cellular Convection and Heat Transport in a Porous Medium', *Applied Science Research*, **39** (1982), p. 21.
- [24] R. Friedrich and N. Rudraiah, 'Numerical Study of Large Amplitude Convection in a Rotating Fluid Saturated Porous Layer', *Proceedings of the Fourth GAMM-Conference on Numerical Methods in Fluid Mechanics*, ed. Henri Viviani. Berlin: Fried Vieweg and Son, 1982, p. 117.
- [25] J. L. Beck, 'Convection in a Box of Porous Material Saturated with Fluid', *Physics of Fluids*, **15** (1982), p. 1372.
- [26] P. H. Forchheimer, 'Wasserbewegung Durch Boden', *Zeitschrift des Vereines Deutscher Ingenieure*, **49** (1901), p. 1736; *ibid.*, **50** (1901), p. 1781.
- [27] N. Rudraiah, M. N. Channabasappa, and G. Ranganna, 'Experimental and Theoretical Study of Non-Darcy Flow Through Porous Media', *4th International Conference on Mathematical Modelling*, Zurich, 1983.
- [28] K. P. Stark and R. E. Volker, 'Nonlinear Flow Through Porous Materials', *Research Bulletin No. 1*, Department of Engineering, University College of Townsville, Australia, 1967.
- [29] C. K. W. Tam, 'The Drag on a Closed Spherical Particles System in Low Reynolds Number Flow', *Journal of Fluid Mechanics*, **38** (1969), p. 537.
- [30] J. C. Slattery, 'Single Phase Flow through Porous Media', *American Institute of Chemical Engineers Journal*, **15** (1969), p. 866.
- [31] W. O. Williams, 'Constitutive Equations for Flow of an Incompressible Viscous Fluid Through a Porous Medium', *Quarterly Journal of Applied Mathematics*, October (1978), p. 255.
- [32] N. Rudraiah, B. C. Chandrasekhara, R. Veerabhadraiah, and S. T. Nagaraj, 'Some Flow Problems in Porous Media', *Post Graduate Studies in Applied Mathematics, Bangalore, India*, **2** (1979) p. 5.
- [33] K. Vafai and C. L. Tien, 'Boundary and Inertia Effects on Flow and Heat Transfer in Porous Media', *International Journal of Heat and Mass Transfer*, **24** (1981), p. 195.
- [34] K. Yamamoto and N. Iwamura, 'Flow with Convective Acceleration Through a Porous Medium', *Journal of Engineering Mathematics*, **10** (1976), p. 41.
- [35] H. C. Brinkman, 'A Calculation of Viscous Force Exerted by a Flowing Fluid on a Dense Swarm of Particles', *Applied Science Research*, **A1** (1947), p. 27.
- [36] N. Rudraiah, 'Coupled Parallel Flows in a Channel and a Bounding Porous Medium of Finite Thickness', *Post Graduate Studies in Applied Mathematics, Bangalore, India*, **5** (1983). (Submitted for publication in the *American Society of Mechanical Engineers Journal of Fluid Engineering*.)
- [37] R. P. Prabhmani and N. Rudraiah, 'Stability of Hydromagnetic Thermoconvection Flow through a Porous Medium', *Transactions of the American Society of Mechanical Engineers Journal of Applied Mechanics*, **E40**, No. 4 (1973), p. 879.
- [38] G. Rohiñi, 'Stability of Flows Through Porous Media', *Ph.D. Thesis*, Bangalore University, 1978.
- [39] N. Rudraiah, B. Veerappa, and S. Balachandra Rao, 'Effects of Non-Uniform Temperature Gradient and Adiabatic Boundaries on Convection in Porous Media', *American Society of Mechanical Engineers, Journal of Heat Transfer*, **102**, No. 2 (1980), p. 254.
- [40] N. Rudraiah, B. Veerappa, and S. Balachandra Rao, 'Convection in a Fluid Saturated Porous Layer with Non-Uniform Temperature Gradient', *International Journal of Heat and Mass Transfer*, **25** (1982), p. 1147.
- [41] N. Rudraiah and S. Balachandra Rao, 'Study of Nonlinear Convection in a Sparsely Packed Porous Medium Using Spectral Analysis', *Applied Science Research*, **40** (1983), p. 223.
- [42] G. S. Beavers and D. D. Joseph, 'Boundary Condition at a Naturally Permeable Bed', *Journal of Fluid Mechanics*, **30** (1967), p. 197.
- [43] N. Rudraiah and T. Masuoka, 'Asymptotic Analysis of Natural Convection through Horizontal Porous Layer', *International Journal of Engineering Science*, **20** (1982), p. 27.
- [44] J. T. Stuart, 'On the Cellular Patterns in Thermal Convection', *Journal of Fluid Mechanics*, **33** (1964), p. 481.
- [45] W. V. R. Malkus and G. Veronis, 'Finite Amplitude Cellular Convection', *Journal of Fluid Mechanics*, **4** (1958), p. 225.
- [46] H. L. Kuo and G. W. Platzman, 'A Normal Mode Nonlinear Solution of the Rayleigh Convection Problem', *Beitrage zur Physik der Atmosphere*, **33** (1961), p. 137.
- [47] R. Friedrich and N. Rudraiah, 'Thermal Convection in a Rotating Fluid Saturated Porous Layer Using Brinkman's Model', presented at Euromech 159, 'Spectral Methods in Computational Fluid Mechanics', Nice, 14-16 September 1982.
- [48] L. F. Shampine and M. K. Gordon, 'Computer Solution of Ordinary Differential Equations', *The Initial Value Problem*. San Francisco: Freeman Publications, 1975.
- [49] N. Rudraiah and S. Balachandra Rao, 'Nonlinear Cellular Convection and Heat Transport by a Rapidly Convergent Solution', *Applied Science Research*, 1983. (Submitted for publication.)
- [50] N. Rudraiah, 'Nonlinear Interaction of Magnetic Field and Convection in Three-Dimensional Motion', *Astronomical Society of Japan*, **33** (1981), p. 721.

**Paper Received 2 November 1983; Revised 14 November 1983.**